Evidence for Apoplasmic Phloem Unloading in Developing Apple Fruit[1]

Ling-Yun Zhang[2], Yi-Ben Peng[2], Sandrine Pelleschi-Travier[2,3], Ying Fan, Yan-Fen Lu, Ying-Min Lu, Xiu-Ping Gao, Yuan-Yue Shen, Serge Delrot, and Da-Peng Zhang*

China State Key Laboratory of Plant Physiology and Biochemistry, China Agricultural University, 100094 Beijing, China (L.Y.Z., Y.B.P., Y.F., Y.F.L., Y.M.L., X.P.G., Y.Y.S., D.P.Z.); and Unité Mixte de Recherches–6161, Centre National de la Recherche Scientifique, 86022 Poitiers, France (S.P.T., S.D.)

The phloem unloading pathway remains unclear in fleshy fruits accumulating a high level of soluble sugars. A structural investigation in apple fruit (*Malus domestica* Borkh. cv Golden Delicious) showed that the sieve element-companion cell complex of the sepal bundles feeding the fruit flesh is symplasmically isolated over fruit development. ^{14}C-autoradiography indicated that the phloem of the sepal bundles was functional for unloading. Confocal laser scanning microscopy imaging of carboxyfluorescein unloading showed that the dye remained confined to the phloem strands of the sepal bundles from the basal to the apical region of the fruit. A 52-kD putative monosaccharide transporter was immunolocalized predominantly in the plasma membrane of both the sieve elements and parenchyma cells and its amount increased during fruit development. A 90-kD plasma membrane H^+-ATPase was also localized in the plasma membrane of the sieve element-companion cell complex. Studies of [^{14}C]sorbitol unloading suggested that an energy-driven monosaccharide transporter may be functional in phloem unloading. These data provide clear evidence for an apoplasmic phloem unloading pathway in apple fruit and give information on the structural and molecular features involved in this process.

The partitioning of sugars in economically important sink organs such as fruits or seeds is governed by several complex physiological processes, including photosynthetic rate, phloem loading in the source leaf, long-distance translocation in the phloem, phloem unloading in sink organs, postphloem transport, and metabolism of imported sugars in sink cells (Oparka, 1990; Patrick, 1997). It is now well accepted that phloem unloading plays a key role in the partitioning of photoassimilate (Fisher and Oparka, 1996; Patrick, 1997; Viola et al., 2001). The process of phloem unloading has been studied extensively over the last 20 years (for review, see Oparka, 1990; Patrick, 1997; Schulz, 1998) but still remains poorly understood. Elucidation of the cellular pathway of phloem unloading is central to this process, because, to a large extent, the unloading path determines the key transport events responsible for assimilate movement from the sieve elements (SEs) to the recipient sink cells (Fisher and Oparka, 1996; Patrick, 1997). A symplasmic phloem unloading pathway predominates in most sink tissues such as vegetative apices (Oparka et al., 1995; Patrick, 1997; Imlau et al., 1999), sink leaves (Roberts et al., 1997; Imlau et al., 1999; Haupt et al., 2001), and potato tubers that represent a typical terminal vegetative storage sink (Oparka and Santa Cruz, 2000; Viola et al., 2001). Symplasmic unloading is also efficient in the maternal tissues of developing seeds that represent a class of terminal reproductive storage sinks (Ellis et al., 1992; Patrick et al., 1995; Wang et al., 1995a; Patrick, 1997), although transfer of solutes to the apoplasm may occur at some point along the postphloem pathway (Patrick, 1997). In some cases, symplasmic unloading also occurs in elongating zones of the stem and in the mature axial path where radial transport of assimilates from the phloem may follow sym- or apoplasmic routes (Hayes et al., 1987; Schmalstig and Cosgrove, 1990; Oparka et al., 1995; Patrick and Offler, 1996; van Bel, 1996; Wright and Oparka, 1997). The predominance of a symplasmic unloading pathway is associated with greater transport capacity and lower resistance (Patrick and Offler, 1996; Patrick, 1997). The unloading route may differ according not only to sink types, but also to sink development, sink function, and even to growth conditions for a particular sink type, and alternative unloading pathways may exist in the sinks with symplasmically interconnecting phloem (Patrick,

[1] This work was supported by China National Natural Science Foundation (grant nos. 30070532, 30270919, and 30330420 to D.P.Z.) and by China National Key Basic Research Program (grant nos. G1999011700 and 2003CB114302 to D.P.Z.).

[2] These authors contributed equally to the paper.

[3] Present address: Unité Mixte de Recherches, Laboratoire Morphogénèse des Ligneux, Université d'Angers, Institut National de la Recherche Agronomique, 2 Boulevard Lavoisier, 49045 Angers, France.

* Corresponding author; e-mail zhangdp@sohu.net; fax 86–10–62891899.

Article, publication date, and citation information can be found at www.plantphysiol.org/cgi/doi/10.1104/pp.103.036632.

1997; Roberts et al., 1997; Oparka and Turgeon, 1999; Viola et al., 2001). These observations are supported by recent research revealing that the plasmodesmal conductivity can be programmatically reduced (Baluska et al., 2001; Itaya et al., 2002) and that the transgenic expression of both apoplasmic invertase (Sonnewald et al., 1997) and sugar transporter (Harrison, 1996; Kuhn et al., 2003) may occur in tissues characterized by a predominant symplasmic phloem pathway. Because of the probable limitations due to transmembrane solute movement, apoplasmic phloem unloading is theoretically scarcely realizable in strong sinks such as meristems, seeds, and fruits (Offler and Patrick, 1993; Wang et al., 1995b).

The mechanism of phloem unloading has been studied in vegetative sinks and developing seeds. However, in fleshy fruits, which are the other class of terminal reproductive strong storage sinks, this mechanism has received little attention. The phloem unloading has been studied in tomato fruit, in which a symplasmic pathway operates at early stages, but an apoplasmic pathway occurs later during fruit development (Fieuw and Willenbrink, 1991; Ruan and Patrick, 1995; Patrick and Offler, 1996). Among the fleshy fruits that, unlike tomato, accumulate high concentrations of soluble sugars, only citrus fruit and grape berry have been studied. In citrus fruit, disruption of the symplasmic continuity within the stalks of juice vesicles and ^{14}C-assimilate tracing provided some evidence for apoplasmic postphloem transport (Koch and Avigne, 1990). In grape berry, the high sugar concentrations in the berry apoplast and their

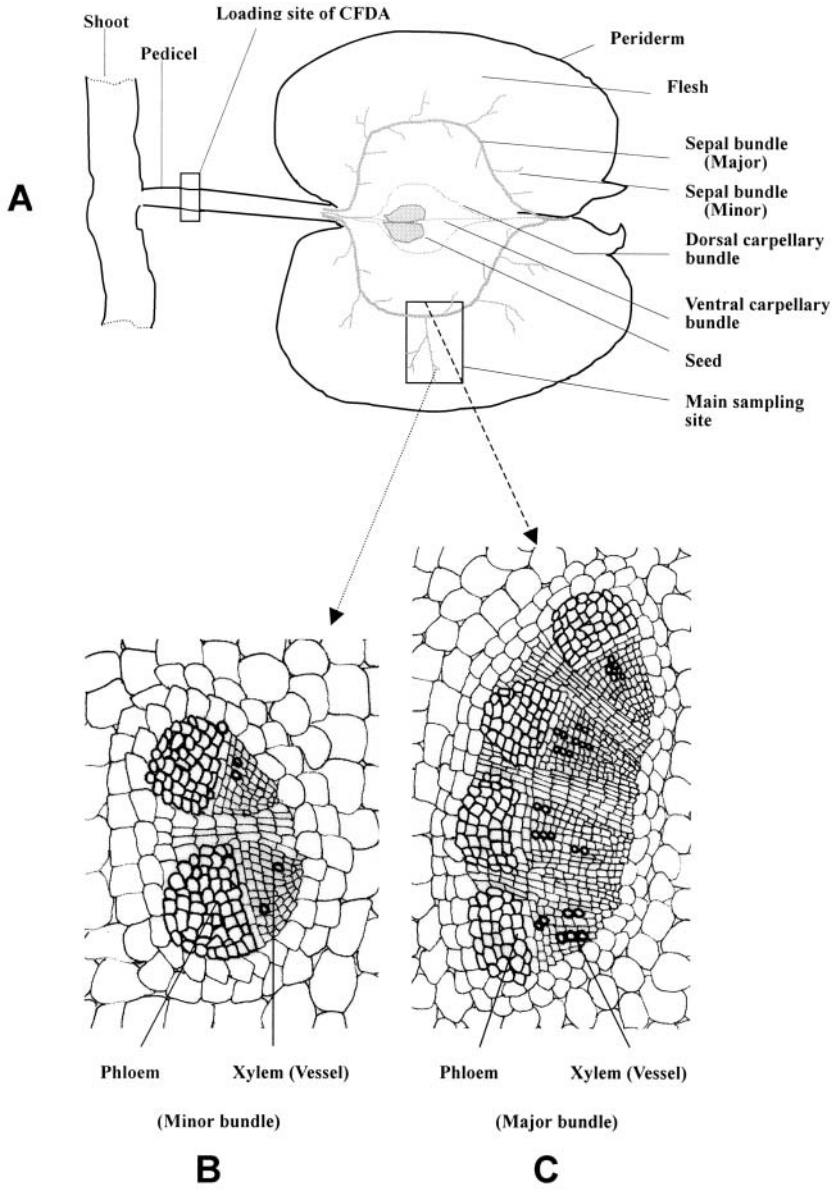

Figure 1. Anatomy of apple fruit, main sampling site and site of CFDA introduction into the fruit pedicel. A, Longitudinal section of apple fruit, showing the network of the vascular bundles of different origins and the loading site of CFDA into the pedicel. B and C, Anatomical sections of the minor and major sepal bundles, respectively.

sensibility to changes in phloem import rate suggest an apoplasmic mode of phloem unloading (Brown and Coombe, 1985; Lang and During, 1991; Patrick, 1997).

Apple fruit (*Malus domestica*) is one of the economically important sink organs in which sugar accumulation is a major determinant of yield and quality. This study aims at a better insight into the phloem unloading pathway in apple fruit. We report that the SE-companion cell (CC) complex is symplasmically isolated over the fruit development, and that 6(5)carboxyfluorescein (CF), a phloem mobile symplasmic tracer, is transported along the functional phloem strands without diffusion. In addition, a putative monosaccharide transporter and an isoform of H^+-ATPase are immunolocalized in the plasma membrane of SE-CC complex, and their possible function in phloem transport is tested by studies of [^{14}C]sorbitol unloading in vivo.

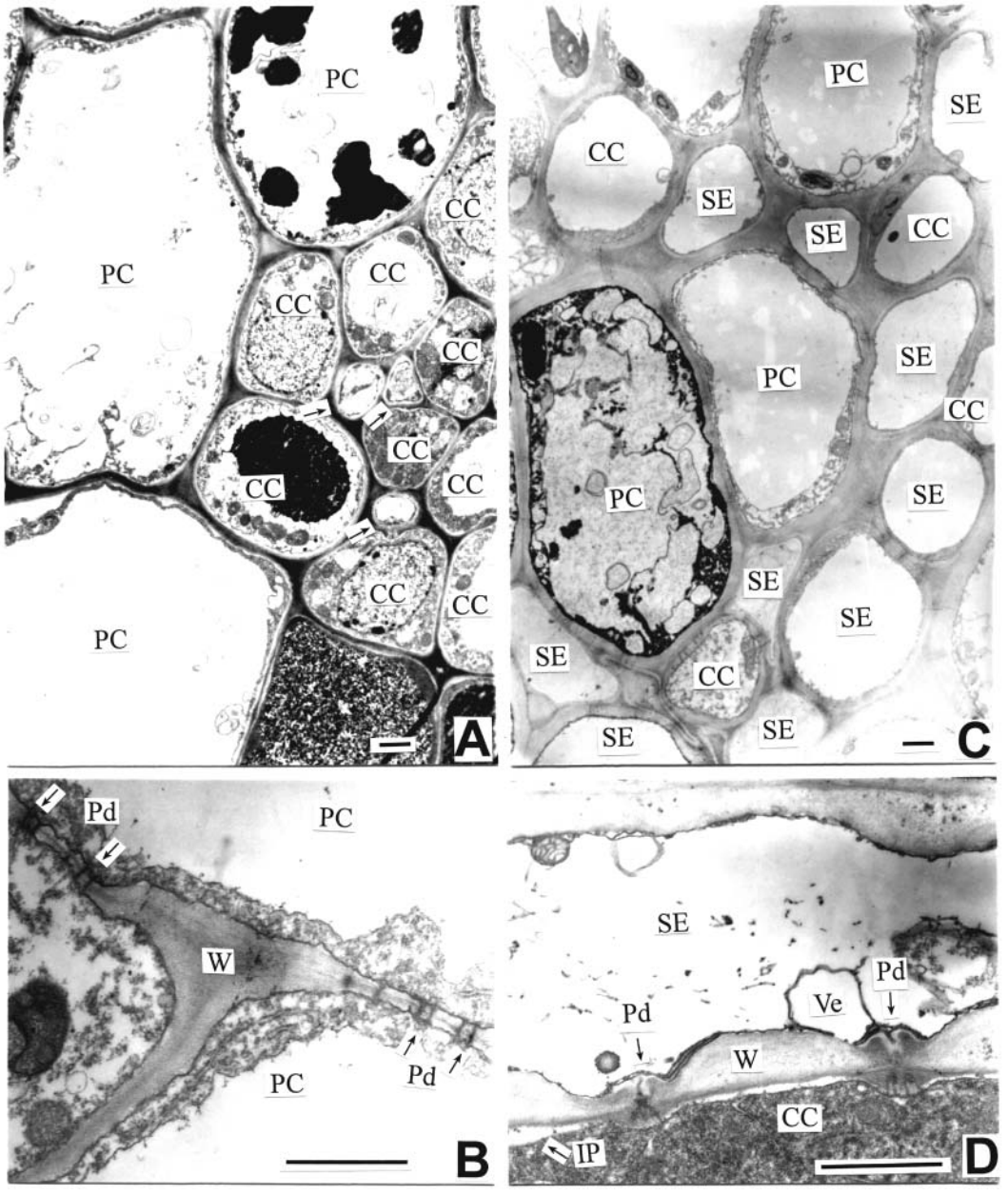

Figure 2. The ultrastructure of SE-CC complex in the major and minor sepal bundles of apple fruit (sampled at the early developmental stage). A, A transverse section of the phloem in the minor bundle. Arrows indicate SEs. B, Numerous plasmodesmata present between PCs. C, A transverse section of the phloem in the major bundle. D, A longitudinal section of SE-CC complex in the major bundle. Note branched plasmodesmata between SE and CC. Bars = 1 μm. CC, companion cell; IP, incipient plasmolysis; PC, parenchyma cell; Pd, plasmodesma; SE, sieve element; SE-CC complex, sieve element-companion cell complex; Ve, vesicle; W, cell wall.

Table I. *Plasmodesmal densities (PDD) and frequencies (PDF) between different cells in phloem of the major and minor sepal bundles of developing apple fruit during the early, middle, and late developmental stages*

SE, sieve element; CC, companion cell; PC, parenchyma cells. Unit of PDD and PDF, number of plasmodesmata μm^{-2}.

Stages	Bundles	SE/CC		SE/PC		CC/PC		PC/PC	
		PDD	PDF	PDD	PDF	PDD	PDF	PDD	PDF
Early	Major	2.96	2.00	0.05	0.05	0.05	0.05	2.98	3.00
	Minor	3.00	2.50	0.00	0.00	0.00	0.00	2.88	2.35
Middle	Major	2.90	2.05	0.03	0.02	0.03	0.02	2.95	3.00
	Minor	2.96	2.53	0.00	0.00	0.00	0.00	2.90	2.40
Late	Major	3.00	2.30	0.00	0.00	0.00	0.00	3.00	2.95
	Minor	3.00	2.45	0.00	0.00	0.00	0.00	2.90	2.95

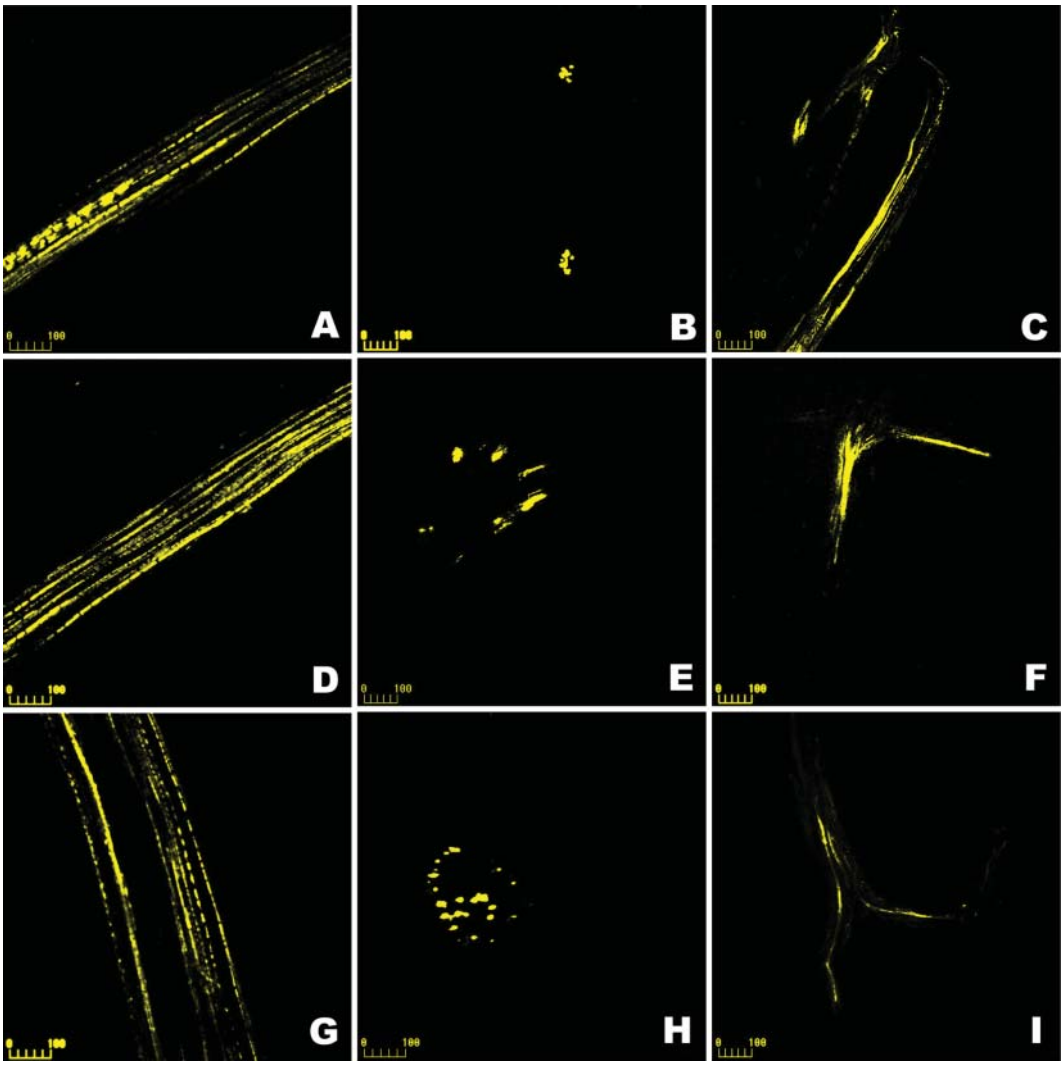

Figure 3. CLSM imaging of CF unloading during development of apple fruit. CF reached the fruit flesh phloem 4 h after loading of the pedicel. The treated fruit was sampled 72 h after CF loading, and the hand-sections were prepared from the sepal bundle zone in the central area (indicated in Fig. 1A and Fig. 4A0 as main sampling site). A–C, Fruit collected at the early stage. A, Phloem strand in the major bundle; B, Transverse section view of two phloem strands in the minor bundles near the apex of fruit (sepal scar side); C, Branched phloem strand in the minor bundle with its extremities. D–F, Fruit collected at the middle stage. D, Phloem strand of the major bundle; E, Transverse section view of phloem strand of the major bundle; F, Branched phloem strand of the minor bundle with its extremities. G–I, Fruit collected at the late stage. Longitudinal (G) and transverse (H) section of the phloem strand of the major bundle; I, Branched phloem strands of the minor bundle with their extremities. Bars = 100 μm.

RESULTS

Structurally Symplasmic Isolation of SE-CC Complex

Apple fruit is a typical pseudocarpous fruit. The fleshy portion largely originates from the perianth, so that the developing flesh of apple fruit is fed with photoassimilates through the sepal vascular bundles (Dennis, 1986; see also Fig. 1A). Our previous investigation, which concerned only the major sepal bundle, showed that the plasmodesmatal frequency between the SE-CC complex and its adjacent cells was low in the major bundle at the early stage of fruit development (Zhang et al., 2001b). The present study shows that the major and minor sepal bundles differ in both their size and structure with more vascular strands and xylem vessels in the major than in the minor bundles (Fig. 1, B and C). The vessels even disappear at the extremity of the minor bundle (data not shown). The SEs are smaller than the CCs in the minor bundle (Fig. 2A), but their size is similar to that of CCs in the major bundle (Fig. 2C). Plasmodesmata are numerous between parenchyma cells (PCs) including phloem and storage parenchyma (Fig. 2B; Table I), and at the interface between SE and CC (Fig. 2D; Table I). However, plasmodesmata were scarcely observed at the interface between the SE-CC complex and its adjacent PCs (Fig. 2, A and C; Table I). The results obtained in the major bundle at the early stage

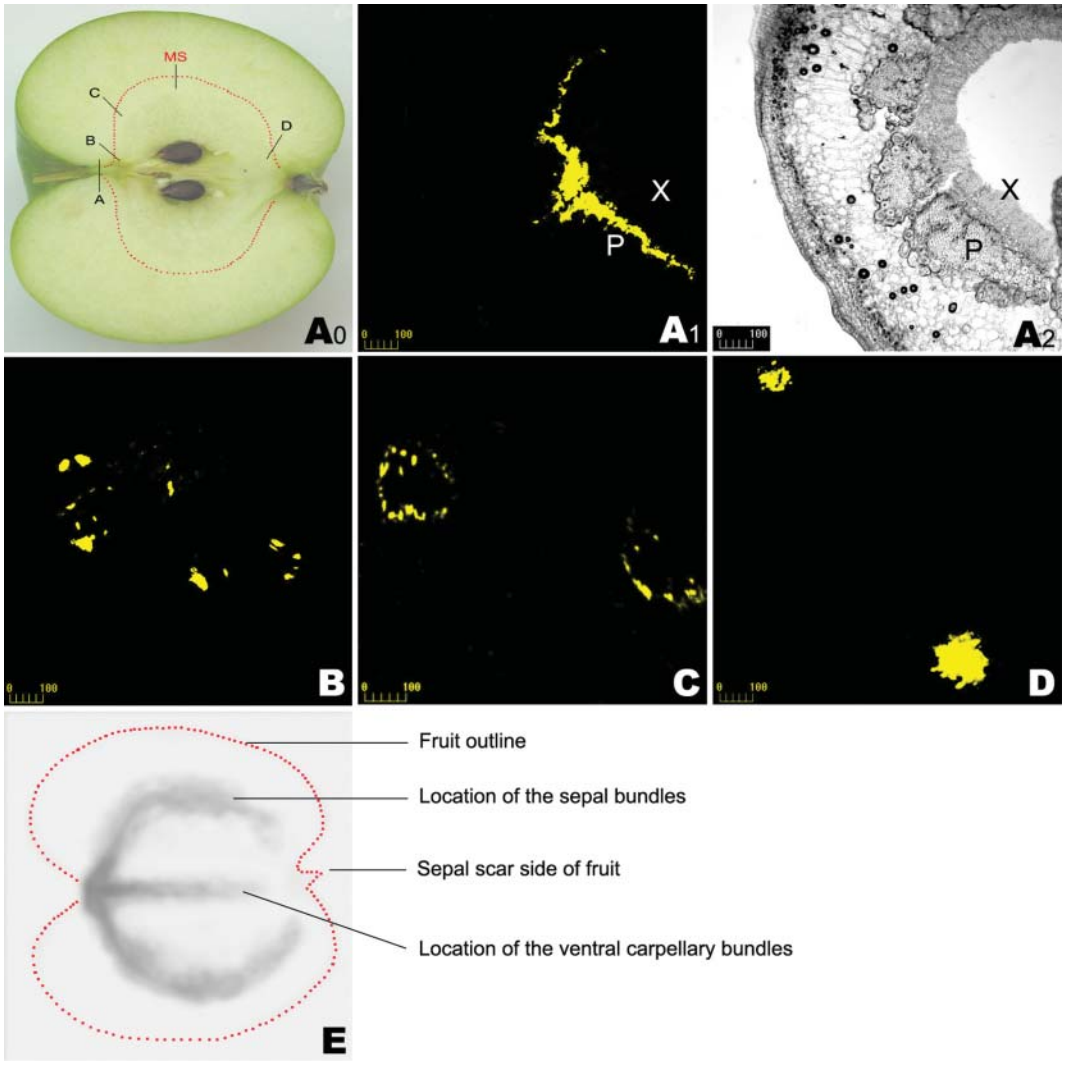

Figure 4. CF CLSM imaging shown by serial transverse sections throughout whole fruit and ^{14}C-autoradiography at the late developmental stage. CF reached the phloem of the fruit flesh 4 h after being supplied to the fruit pedicel. The treated fruit was harvested 72 h after CF supply. A0, Longitudinal section of apple fruit showing the sampling locations for A1, A2, B, C, and D. A1, CLSM imaging in the transverse section of a portion of the CF-loaded pedicel close to the fruit flesh (see A0), showing that CF was restricted to the phloem zone of the vascular bundle. The corresponding bright-field image is shown in A2. B–D, CLSM imaging of CF in the transverse sections at the different points in fruit (see A0 for the locations of B, C, and D). E, ^{14}C-unloading is apparent along the sepal bundles and the ventral carpellary bundles in fruit. MS in the Figure A0, main sampling site for CLSM imaging at different stages of fruit development, as indicated in Figure 1A; P, phloem; X, xylem. Bars = 100 μm (for Fig. 4, A1–D).

are consistent with those previously reported (Zhang et al., 2001b). In the major bundle, the plasmodesmal density and frequency become null at the late stage of fruit development, whereas in the minor bundle they are null throughout the fruit developmental process (Table I).

CF Is Confined to Functional Phloem Strands

When it is loaded into cells, the membrane-permeable and nonfluorescent CF diacetate (CFDA) is degraded to CF, a membrane-impermeable fluorescent dye. CF is often used as a fluorescent marker of phloem transport and symplasmic phloem unloading (Roberts et al., 1997), and its behavior is similar to the pattern of assimilate unloading determined by autoradiography (Viola et al., 2001). Preliminary experiments showed that CF supplied to the apple fruit pedicel reached the fruit flesh about 4 h after CF loading, which is in good agreement with the transport velocity of [^{14}C]Suc. Furthermore, the unloading route of CF remained the same thereafter, even when the samples were collected 120 h after CF application (data not shown). Confocal laser scanning microscopy (CLSM) images of CF movement in the fruits sampled 72 h after CF supply to the pedicel (68 h after CF arrival into the fruits) are presented in Figure 3. A series of experiments conducted during the growing season showed that CF was always confined to the phloem strands along the phloem pathway in the sepal bundles without apparent diffusion to the surrounding tissues. This held true for major and minor bundles in straight or branched regions, either in transverse or longitudinal sections, at the early (Fig. 3, A–C), middle (Fig. 3, D–F), and late (Fig. 3, G–I) stages of fruit development. A survey of CF unloading by serial transverse sections along the whole fruit confirmed the above observations. CF was restricted to the phloem strands along the sepal bundle throughout the fruit from the basal (pedicel side) to the apical (sepal scar side) region (Fig. 4, A–D). After feeding $^{14}CO_2$ to the spur leaves, ^{14}C-assimilates were apparently unloaded from the sepal and carpellary bundles in fruit (Fig. 4E), revealing that the phloem of these bundles was functional for unloading.

A Monosaccharide Transporter, Expressed Increasingly with Fruit Development, Is Localized to Plasma Membrane of Both SEs and PCs

To analyze the expression of monosaccharide transporters, immunoblotting with the antiserum raised against the putative grape hexose transporter VvHT1 (Fillion et al., 1999) was carried out in different subcellular fractions of the fruit flesh, and the protein was further immunolocalized on ultrathin sections of embedded material with this heterologous antiserum. The anti-VvHT1 serum recognized a single polypeptide in the plasma membrane fraction of the fruit flesh, with an apparent molecular mass of approximately 52 kD (Fig. 5A), which is similar to that of the grape hexose transporter (48.4 kD). No immunosignal was detected in the endomembrane or cytosolic fractions (Fig. 5A). The amount of the 52-kD polypeptide increased throughout fruit development (Fig. 5A).

Immunogold labeling conducted from the early to late stage of fruit development with anti-VvHT1 serum showed that the putative monosaccharide transporter protein predominantly localized to the plasma membranes of SEs and of their surrounding PCs (including phloem and flesh storage parenchyma) at all the developmental stages (Fig. 6, A–F). In CC, however, the density of immunogold particles was lower than in SE or PC (Fig. 6, A–F; Table II). The density of the plasmalemma-localized immunogold particles in SE was substantially the same as in PC at the early stage of fruit development (Fig. 6, A and B; Table II), but it became higher in SE than in PC at the middle and late stages (Fig. 6, C–F; Table II). No significant difference, however, was found between SEs in the phloem of the major and minor bundles (Table II). The amount of putative monosaccharide transporter increased from the early to the late stages of fruit development (Fig. 6, A–F; Table II), whether in SE, PC, or even CC (Table II), which is consistent with the immunoblot results. Importantly, no gold particles were found in any of the controls without the antiserum (Fig. 6, G and H), or with the preimmune serum controls (data not shown), indicating that the

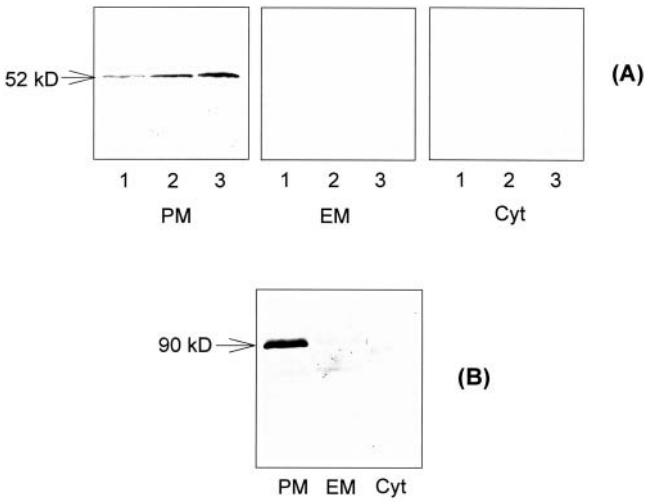

Figure 5. Immunoblotting of putative monosaccharide transporter (A) and H^+-ATPase (B) in apple fruit. A, Immunoblotting with anti-VvHT1 serum. A 52-kD polypeptide was detected in plasma membrane (PM) of the fruit flesh harvested at the early (lane 1), middle (lane 2), and late (lane 3) stages of fruit development, but no immunosignal was observed in endomembranes (EM) or cytosolic fraction (Cyt). Fifty micrograms of protein was loaded in each lane. B, Immunoblotting with anti-AHA3 serum. A 90-kD polypeptide was detected in plasma membranes (PM) at the early stage of fruit development, but no immunosignal was found in endomembranes (EM) or cytosolic fraction (Cyt). Four micrograms of protein was loaded in each lane.

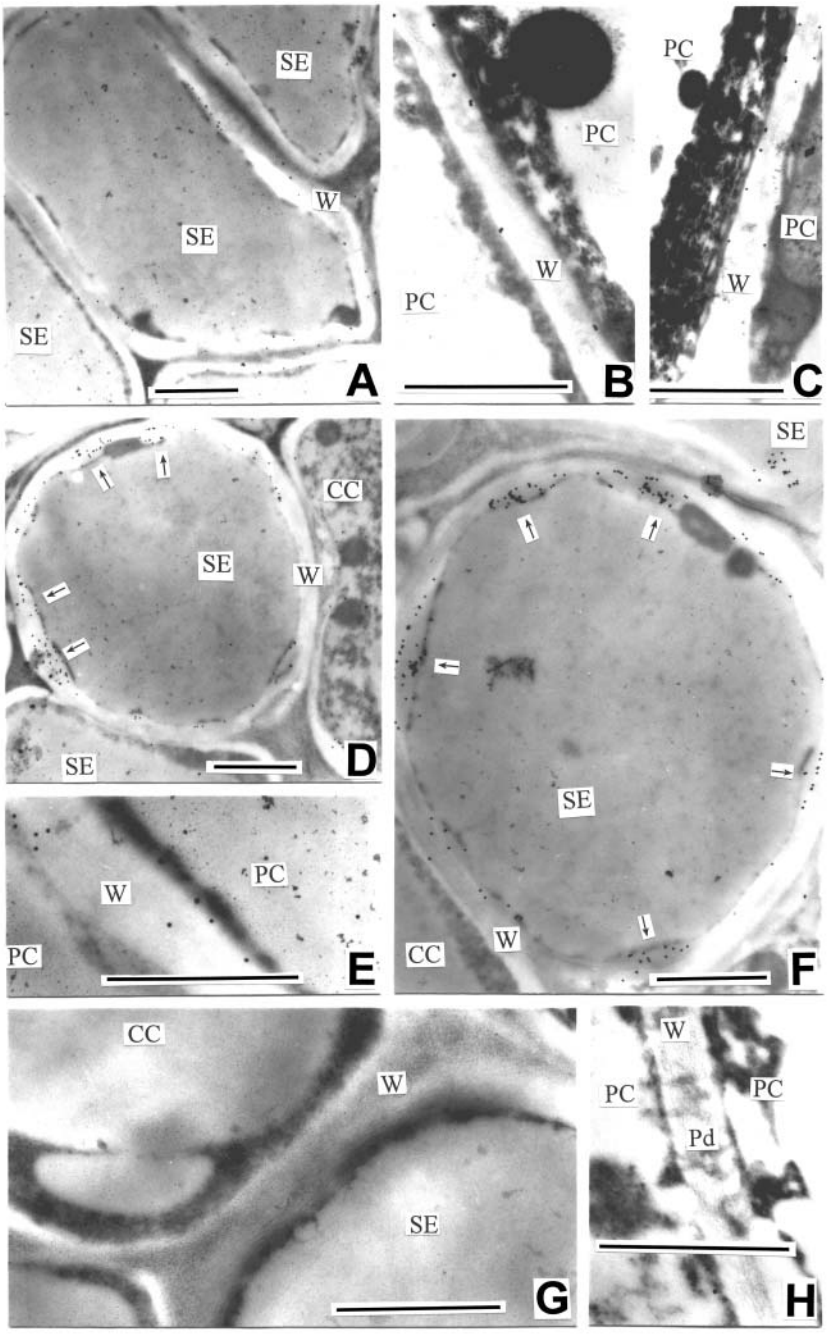

Figure 6. Immunogold localization of putative monosaccharide transporter in the flesh of apple fruit. The protein reacting with anti-VvHT1 serum mainly resides in the plasma membrane of SEs and is also found in the plasma membrane of PCs at the early (A, SEs; B, PCs), middle (C, PCs; D, SEs) and late (E, PCs; F, SEs) stages of fruit development. Note that there are much fewer transporter molecules in the plasma membrane of CCs (D, F). The number of immunogold particles apparently increases from the early to late developmental stages in the plasma membrane of SEs. The immunogold particles were scarcely found in the cytoplasm or vacuole of SE or PC (A–F). G and H, SE-CC complex (G) and PCs (H) in a control without antiserum. No substantial signal was detected. Bars = 1 μm. Abbreviations are as in Figure 2.

antiserum was specific and that unspecific labeling was negligible.

H^+-ATPase in the SE-CC Complex

Immunoblotting with the antiserum against Arabidopsis plasma membrane H^+-ATPase AHA3 (Pardo and Serrano, 1989) revealed a 90-kD polypeptide in the plasma membrane fraction of apple fruit (Fig. 5B), while no immunosignal was detected in the endomembrane or cytosolic fractions (Fig. 5B). Further immunogold localization of H^+-ATPase conducted with the same antiserum clearly detected the enzyme in the plasma membrane of SE-CC complex (Fig. 7, A and B). No substantial immunosignal was detected in the control without antiserum (Fig. 7C), and that using the preimmune serum control (data not shown), indicating that the H^+-ATPase immunolocalization was specific and reliable.

Physiological Evidence for an Energy-Driven Monosaccharide Transporter

In apple, as in other species of Rosaceae, sorbitol and Suc are the major translocated sugars, with the sorbitol concentrations in the phloem being higher than the

Table II. *Density of gold particles (number μm^{-2}) representing putative monosaccharide transporters on plasma membranes in fruit cells during the early, middle, and late developmental stages*

The gold particles were counted on 10 ultrathin sections for each sample, and the values below are the means ±SD (n = 10). SE, sieve element; CC, companion cell; PC, parenchyma cells.

Stages	Major Bundle		Minor Bundle		PC
	SE	CC	SE	CC	
Early	4.1 ± 0.5	0.6 ± 0.1	4.2 ± 0.4	0.5 ± 0.1	4.0 ± 0.5
Middle	9.2 ± 1.5	1.0 ± 0.3	9.0 ± 1.5	0.9 ± 0.2	6.1 ± 0.7
Late	15.0 ± 2.0	2.0 ± 0.5	15.6 ± 0.2	2.0 ± 0.5	8.5 ± 1.2
Average	9.4	1.2	9.6	1.1	6.2

Suc concentrations (Loescher, 1987). To assess whether a monosaccharide transporter and plasma membrane H^+-ATPase are involved in phloem transport of sugars in apple fruit, the effects of various chemicals on [^{14}C]sorbitol unloading were assayed. The chemical reagents were introduced into the fruit flesh from the wells made into the fruits (Fig. 8, A and B) by an unloading trap technique used previously in our laboratory (Lu et al., 1999). A mild enzymatic digestion of the flesh cell wall portions from the wells was conducted in order that the effector macromolecules could easily reach the plasma membranes. This treatment did not significantly affect the [^{14}C]sorbitol unloading (Fig. 8, C and D), indicating that this experimental system was reliable. It is noteworthy that, in this system, [^{14}C]sorbitol unloading was measured both in the flesh cells and in the apoplasmic space of the flesh. The radioactivity accumulated in the flesh cells was measured with the digested well-tissues that were washed after sampling, and the unloading in the apoplasmic space with the unloading medium placed in the wells. Treatments of the well-tissues by the sulfhydryl group modifier p-chloromercuribenzenesulfonic acid (PCMBS), the plasma membrane H^+-ATPase inhibitor Na_3VO_4, anti-VvHT1 or anti-AHA3 serum significantly reduced the [^{14}C]sorbitol unloading into both the apoplasmic space and the flesh cells, with a stronger inhibition by PCMBS and Na_3VO_4 than by the two antisera (Fig. 8, C and D). This held true throughout the experimental period tested (5–6 h, 7–8 h, and 9–10 h after [^{14}C]sorbitol feeding from the pedicel). Treatments with rabbit preimmune serum induced no inhibition (Fig. 8, C and D), indicating that the effects of the two antisera were specific. These results suggested that a functional monosaccharide transporter, driven by H^+-ATPase activity, is involved in phloem unloading of sugars in apple fruit.

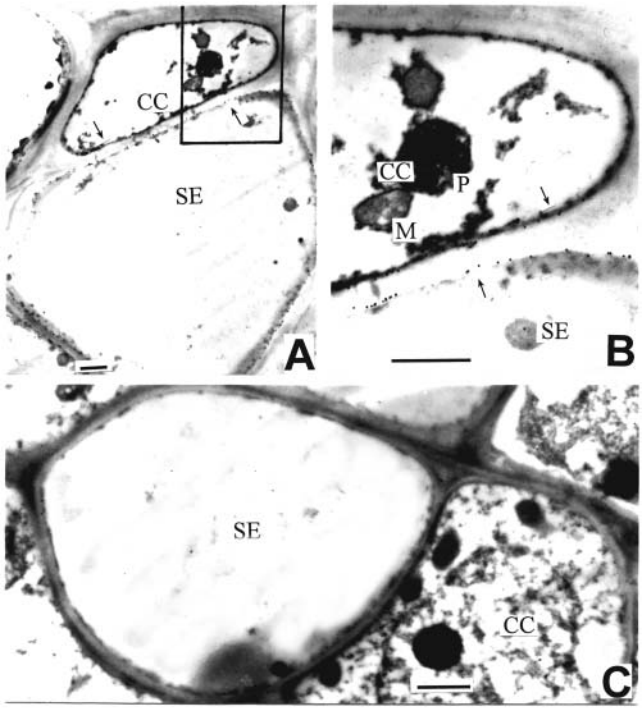

Figure 7. Immunogold localization of H^+-ATPase in SE-CC complex of apple fruit at the early stage of development. A, Immunogold localization of H^+-ATPase in SE-CC complex. Immunogold particles are present in the plasma membrane (indicated by arrows) of the SE-CC complex. B, Blow-up of the area shown in A. C, Control without antiserum in SE-CC complex. Bars = 1 μm. P, plastid. Other abbreviations are as in Figure 2.

DISCUSSION

Phloem Unloading Follows an Apoplasmic Pathway in Apple Fruit

The present cytological and physiological studies reveal that the SE-CC complex in the phloem of sepal vascular bundles feeding the fruit flesh with assimilates is symplasmically isolated. This was shown first by the complete absence of plasmodesmata at the interface between the SE-CC complex and its surrounding cells over apple fruit development (Fig. 2; Table I). Furthermore, an in vivo functional investigation of CF movement by CLSM showed that the dye is confined strictly to phloem strands in the fruit flesh (Figs. 3 and 4). Autoradiographs (Fig. 4) indicated that the phloem strands are functional for assimilate unloading. These different approaches provide clear evidence for an extensive apoplasmic phloem unloading pathway in apple fruit, namely, in the major and

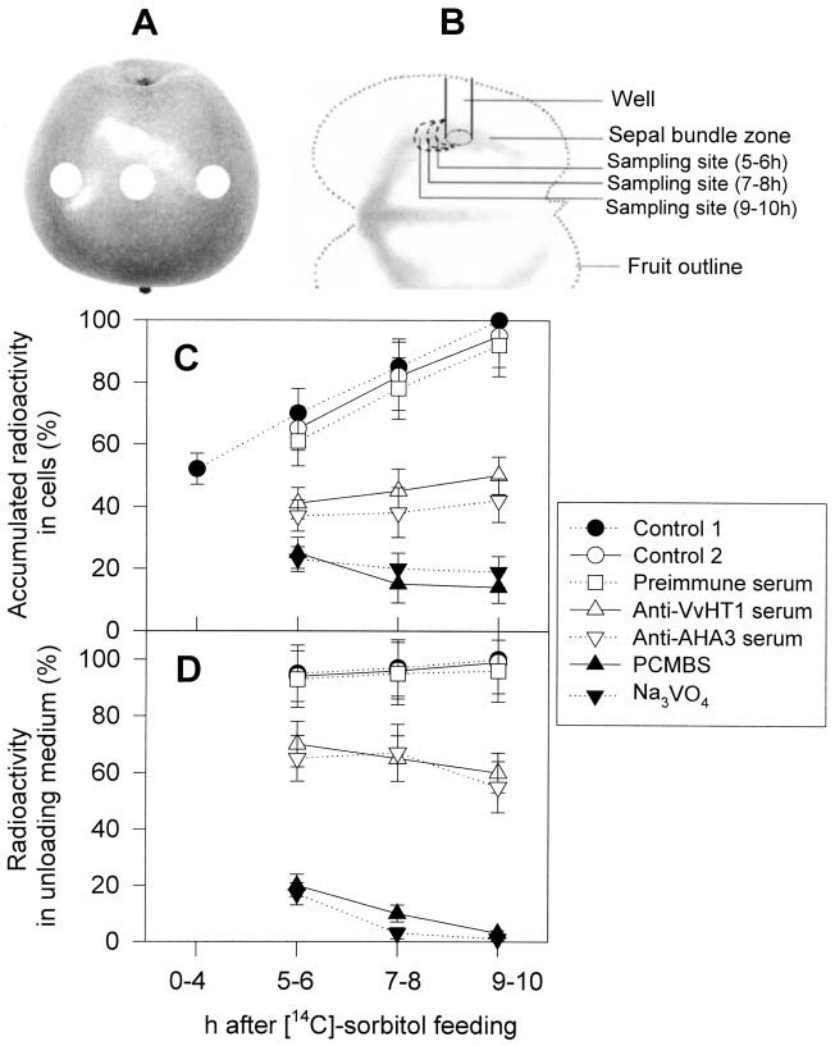

Figure 8. Effects of some inhibitors and antisera on [^{14}C]sorbitol unloading. Fruits were continuously fed with [^{14}C]sorbitol from the pedicel, and the effectors were introduced from the wells (unloading trap) made into the fruits as described in ''Materials and Methods''. A, The circles marked on the fruit indicate the positions of the wells. B, Diagram showing the positions of the wells in the longitudinal section of the fruit and the sampling sites in the wells for radioactivity measurements shown in C and D. [^{14}C]sorbitol unloading was evaluated in the flesh cells (the well-tissues washed by the fresh unloading medium) (C) and in the apoplasmic unloading medium (D). The radioactivity at 0 to 4 h in C was measured with the tissues sampled when the wells were made by cork borer 4 h after the [^{14}C]sorbitol feeding. Control 1 represents the wells receiving only the unloading medium, and control 2, the wells subjected to a mild enzymatic digestion and a subsequent treatment by the noneffector-contained buffer A. Radioactivity is expressed as percentages relative to the maximum values obtained with the last sampled tissues (10 h after [^{14}C]sorbitol feeding) of the control 1. The absolute maximum values of radioactivity were 720 ± 215 (Bq/0.5 g tissue) for the well-tissues and 320 ± 125 (Bq/0.5 mL) for the unloading medium. Each percentage was calculated within the same sampling time and in the same set of experiments. Values are means ±SE (n = 7).

minor bundles, from the basal to the apical areas, and throughout the fruit developmental process (Figs. 2–4).

We tried to use 3-kD Texas Red (Molecular Probes, Eugene, OR), a widely used xylem vessel tracer, to distinguish clearly the phloem from xylem, but the dye failed to enter the fruit flesh, which is probably due to a high resistance of the xylem in the pedicel or within the flesh. Indeed, as in other fleshy fruits and developing seeds, the xylem conductivity in apple pedicel significantly declines during fruit development (Lang and Ryan, 1994). In our study, a deficiency and even an absence of vessels in the minor sepal bundles of the flesh were observed (Fig. 1). This hydraulic isolation may be important to prevent the loss of the apoplasmic solutes via the xylem in apple fruit. Nevertheless, CF is a useful symplasmic tracer in apple fruit. CF loading into the pedicel was strictly limited to the phloem, with no apparent diffusion of the tracer into the neighboring zone even 70 h after loading (Fig. 4A). This indicates that the phloem route is a unique path to lead to the vascular bundles of the fruit.

As in the sepal bundles (see above), phloem unloading in the carpellary bundles also followed an apoplasmic pathway (data not shown). It is noteworthy that the phloem of the sepal bundles, especially that of the major sepal bundles, looks like secondary phloem (Fig. 2). The secondary phloem is clearly transport phloem, unlike the typical terminal release phloem that is mostly of primary nature (Kempers et al., 1998). Transport phloem SEs are often symplasmically isolated (Kempers et al., 1998; Knoblauch and van Bel, 1998). The mechanism of photosynthate release from the sieve tubes of transport phloem is currently unknown. The apoplasmic unloading pathway, however, seems linked to the property of fruit flesh to accumulate a high level of soluble sugars. As a matter of fact, the level of total soluble sugars in the phloem of apple pedicel is lower than 100 mM, whereas it reaches more than 930 mM in the cytosol and 400 mM in the apoplasmic space of apple fruit

(Yamaki and Ino, 1992; Beruter et al., 1997). If phloem unloading were symplasmic and driven mainly by bulk flow and passive diffusion via plasmodesmata, this concentration gradient from the phloem to the flesh cells would result in a back diffusion to the SEs (Fisher and Oparka, 1996; Patrick, 1997). The apoplasmic pathway of phloem unloading, together with the hydraulic isolation of the fruit xylem, constitutes an efficient mechanism to hinder the potential back flow out of the fruit. This may be a common feature in the terminal strong storage sinks accumulating a high level of soluble sugars. In these sinks, a mechanism against the back flow of soluble sugars out of the sinks is highly necessary, unlike vegetative sinks such as vegetative apices, stems, roots, sink leaves, and potato tubers, and even reproductive developing seeds where a symplasmic phloem unloading predominates (Patrick, 1997). It is particularly noteworthy that the phloem unloading pathway in apple fruit also differs from that in tomato fruit. In tomato, which accumulates a relatively lower level of soluble sugars, unloading follows a symplasmic route at the early stage and an apoplasmic route at the late stage of fruit development (Fieuw and Willenbrink, 1991; Ruan and Patrick, 1995; Patrick and Offler, 1996).

Possible Mechanism of Phloem Unloading in Apple Fruit

It is currently accepted that assimilate efflux across the plasma membrane of the SE-CC complex involves either simple diffusion down a steep concentration difference or a transporter-mediated and energy-coupled process, or both (Patrick, 1997). Simple diffusion is not possible in apple fruit because the concentration of the soluble sugars is higher in the fruit apoplast than in the phloem (Yamaki and Ino, 1992; Beruter et al., 1997). This suggests a transporter-mediated active process coupled with protons returning down the electrochemical gradient generated by a plasma membrane H^+-ATPase. In the present study, a plasma membrane 52-kD polypeptide reacting with a serum directed against a putative monosaccharide transporter from grape berry was identified (Fig. 5). This 52-kD polypeptide may be considered as a member of the monosaccharide transporter family that shares significant regions of sequence identity among its members and is part of a superfamily of porters evolved from a common ancestor (Buttner and Sauer, 2000). However, given that this family includes hexose transporters and polyol transporters that may have a wide substrate specificity, it is not possible to assess precisely the specificity of the transporter detected in our experiments. Also, a 90-kD polypeptide was detected in the plasma membrane of the fruit flesh cells (Fig. 5) reacting with an antiserum directed against the Arabidopsis plasma membrane H^+-ATPase AHA3. This ATPase is an isoform expressed preferentially in the phloem of both source and sink tissues (Oparka and Turgeon, 1999). The 52-kD putative apple monosaccharide transporter is specifically localized to the plasma membrane of both the SE and PC (Fig. 6; Table II). The 90-kD H^+-ATPase is abundant in the plasma membrane of the SE-CC complex (Fig. 7). The expression of the 52-kD putative monosaccharide transporter increased during fruit development (Figs. 5 and 6; Table II), which coincides with the growing concentrations of sorbitol in the pedicel phloem and of Fru in the fruit flesh (Zhang and Wang, 2002). In addition, in the experiment of [^{14}C]sorbitol unloading in vivo where the reagents were applied to the fruit flesh while [^{14}C]sorbitol was continuously supplied to the pedicel, unloading of [^{14}C]sorbitol into both the apoplasmic space and the fruit flesh cells was significantly inhibited by PCMBS, Na_3VO_4, anti-VvHT1 or anti-AHA3 serum (Fig. 8), suggesting that the 52-kD putative monosaccharide transporter and the 90-kD H^+-ATPase are functionally involved in phloem unloading. Given the absence of substantial immunogold labeling in the CC, these data suggest that unloading of the SE-CC complex may occur across the plasma membrane of the SE rather than that of the CC, and that this process depends both on a H^+-ATPase and on a monosaccharide transporter.

Currently, the phloem unloading is considered as an inverse process of the phloem transmembrane loading mediated by a sugar/proton symporter (Patrick, 1997). However, phloem unloading is an energy-driven process in many sinks as in apple fruit (Lu et al., 1999), which suggests the operation of a sugar/proton antiporter mediating the efflux from phloem (Fieuw and Patrick, 1993). A cDNA encoding a sorbitol transporter was recently cloned from sour cherry fruit (Gao et al., 2003). Further work on the potential role of a similar transporter in apple will be of particular importance to elucidate the mechanism of phloem unloading in this fruit.

Whatever the exact mechanism of phloem unloading in apple fruit, the predominant plasma membrane-localization of both the 52-kD putative monosaccharide transporter and the 90-kD H^+-ATPase in the SE provides additional support for the apoplasmic phloem unloading pathway that is revealed more directly by both the symplasmic isolation of the SE-CC complex and CF confinement to the phloem strands. The predominantly cell wall-localization of invertases (Zhang et al., 2001b) is also in agreement with an apoplasmic phloem unloading pathway in this fruit. Postphloem transport may occur by simultaneous apo- and symplasmic pathways, as indicated by the plasma membrane-located putative monosaccharide transporter in the PCs (Fig. 6) and the numerous plasmodesmata connecting these cells (Fig. 2).

MATERIALS AND METHODS

Plant Material

Apple (*Malus domestica* Borkh. cv Golden Delicious) fruits were sampled throughout the growing season from 8- to 9-year-old trees growing in a commercial orchard in the western suburbs of Beijing. Most samples were

collected at the following developmental stages: early developmental stage (30th day after full bloom when the size of fruit was about 15 g fresh weight/fruit); middle developmental stage (60th day after full bloom when the size of fruit was about 70 g fresh weight/fruit), and late developmental stage (90th day after full bloom when the size of fruit was about 150 g fresh weight/fruit).

Chemicals

Antiserum against Arabidopsis plasma membrane H^+-ATPase AHA3 (Pardo and Serrano, 1989) was a generous gift from Dr. R. Serrano (Universidad Politecnica, Valencia, Spain). Goat anti-rabbit IgG antibody conjugated with 10 nm gold, goat anti-rabbit IgG antibody conjugated with alkaline phosphatase, nitroblue tetrazolium, nitrated cellulose membrane (0.45 μm), and [^{14}C]sorbitol (22.8 GBq mmol^{-1}) were purchased from Amersham Pharmacia Biotech (Little Chalfont, UK). All other chemicals were purchased from Sigma (St. Louis) unless otherwise noted.

Tissue Preparation for Structural Observation

The method described by Zhang et al. (2001b) was used. The vascular bundle zone (sepal bundles including major and minor bundles; Fig. 1A) was cut into small cubes (about 2–3 mm^3) that were immediately fixed with 5% (v/v) glutaraldehyde in 100 mM precooled phosphate buffer (pH 7.0) for 6 h. The penetration of the glutaraldehyde buffer was improved by vacuum pumping. After an extensive rinse with the precooled phosphate buffer (pH 7.0), the tissue cubes were postfixed in 1% (w/v) OsO_4 overnight at room temperature. Following another extensive rinse with the same buffer, the samples were dehydrated through a graded ethanol series (30%–100%) and 100% acetone, and infiltrated for 24 h with Spurr at room temperature. Polymerization was conducted at 68°C for 8 h. Ultrathin sections (approximately 60–90 nm in thickness) were mounted on 100-mesh copper grids coated with 0.3% Formvar film for the ultrastructural observation (JEM-100S transmission electron microscope).

Measurement of Plasmodesmal Density and Frequency

Measurements of plasmodesmal density and frequency were adapted from Kempers et al. (1998). Five-group series of transverse ultrathin sections were prepared from the Spurr-infiltrated flesh samples, in which each group was cut at a distance of approximately 20 μm from the previous one. From each group, six pieces of ultrathin sections were picked at random and put on the copper grids of 100-meshes. Five scopes (each consisting of phloem and its surrounding PCs) were observed from each ultrathin section. Plasmodesmata were counted at all cell interfaces, i.e. the interfaces between SE/CC, SE/PC, CC/PC, and PC/PC (PC includes phloem parenchyma and flesh storage parenchyma) in each selected field. The results of the plasmodesmal counting were given as the number of plasmodesmata per micron of specific cell/cell interface length on transversal section, or on longitudinal section, the former being referred to plasmodesmal density and the latter to plasmodesmal frequency (no. of plasmodesmata μm^{-1}).

CFDA Labeling

The fruits from sunny tree-crown-layer were treated with CFDA solution. Each plant was labeled with approximately100 μL of 1 mg mL^{-1} CFDA aqueous solution (prepared from a stock solution in acetone). The CFDA solution was introduced into the fruit from the pedicel (Fig. 1A) by a cotton thread immersed in a tube at one end and with the other end passing through the phloem zone of the pedicel. Plants were allowed to translocate the CF for 72 h, and the fruit tissues were subsequently sectioned and examined by CLSM. Attempts to introduce CFDA into the fruit from the leaves were conducted by the technique of Roberts et al. (1997). Whether CFDA was introduced from the pedicel or the leaf, the transport pathway in the fruit tissue was the same, but the arrival of CF to the sampling site was observed 4 h after pedicel loading and 16 h after leaf infiltration. These velocities were comparable to that of [^{14}C]Suc transport into the fruit (data not shown). Furthermore, CF sometimes failed to be transferred into the fruits after leaf infiltration, probably because of disconnection of vascular strands. Therefore, the pedicel-CFDA loading method was chosen because of the high-speed of transport and because of its more reliable efficiency.

Tissue Sectioning

The CFDA-treated apple fruits were harvested at selected times and quickly taken to the laboratory with an ice bucket. Prior to CLSM, the phloem of sink tissue was carefully cut into transverse or longitudinal sections that were immersed immediately into 80% (v/v) glycerol to prevent dye loss (for long time preservation, the immersion oil was used).

Microscopy

A Bio-Rad MRC 1024 CLSM (Hemel Hempstead, UK) was used to image CF transport (optimum excitation at 490 nm and emission at 515 nm) as quickly as possible to minimize the dye loss. CF was excited by the 488-nm beam produced by a 25-mW krypton/argon laser.

Preparation of Anti-VvHT1 Serum

A 443-bp cDNA fragment containing the 141-bp 3′ end coding and the poly A region of the putative grapevine hexose transporter *VvHT1* isolated by one of our laboratories (Fillion et al., 1999) was obtained by PCR amplification. The oligonucleotide primers used for PCR were sense (Cterm): 5′TTG CCT GAA TTC AAA GGC AT3′ and antisense (T3) SK plasmid primer. The sense primer contained an *Eco*RI restriction site. After digestion with T4 DNA polymerase, then with *Xba*I, the purified PCR product was cloned into the pMAL-c2 vector (New England Biolabs, St-Quentin-en-Yvelines, France) digested with *Xmn*I and *Xba*I. The construct was used to transform *Escherichia coli* DH5α cells and sequenced to check for in-frame fusion of the Mal E gene and *VvHT1*coding region.

Expression and purification of the fusion protein were performed according the manufacturer's (New England Biolabs) instructions. Expression of the fusion protein was induced using isopropyl β-D-thiogalactopyranoside (IPTG). Cells were lysed on ice by lysozyme and centrifuged to remove insoluble materials. The resulting supernatant was applied to an amylose affinity column and the MBP-VvHT1 fusion protein was eluted. The purified protein appeared as a 48.7-kD band on a SDS-PAGE gel. Purified protein (380 μg) was used for standard immunization protocols and polyclonal antisera production in rabbits (Eurogentec, Angers, France).

The antiserum was enriched in anti-VvHT1 antibodies by adsorption of nonspecific antibodies. For this, *E. coli* DH5α cells transformed with the pmal-VvHT1 vector were grown in the presence of IPTG, and their soluble proteins were extracted. Protein aliquots (6 $\times$ 100 μg) were immobilized by adsorption on 1 cm^2 nitrocellulose filters for 3 h at room temperature with gentle shaking. The filters were then washed for 3 $\times$ 15 min in blocking buffer [5% (w/v) nonfat dried milk in phosphate-buffered saline (PBS1), 0.02% azide and 0.2% Tween 20], and then in PBS. Two filters were added to 3 mL antiserum at room temperature with gentle agitation. After 2 and 4 h, nitrocellulose filters were replaced, and the purification procedure was repeated. After 6 h, the purified anti-MBP-VvHT1 antiserum was transferred in a sterile tube and tested (1:10 to 1:100 dilution in blocking buffer) by western blotting, which showed that the purified antiserum was highly specific.

Immunogold Labeling

Specimen preparation and immunogold labeling were conducted essentially according to Zhang et al. (2001b). The following procedures were carried out at 4°C unless otherwise stated. The apple flesh in the sepal bundle zone including major and minor bundles (Fig. 1A) was cut into small blocks (about 2- to 3-mm^3 cubes) that were immediately fixed with 4% (w/v) paraformaldehyde and 2.5% (v/v) glutaraldehyde in 100 mM precooled PBS1 (pH 7.2) for 4 h and exhausted until tissue blocks had completely soaked into the blocking solution. After three washes in PBS1, the tissue cubes were dehydrated in a graded series of ethanol (30%–100%) and subsequently infiltrated with a mixture of Lowicryl K_4M and ethanol. Polymerization via UV illumination was conducted for 48 h at −20°C and for another 48 h at room temperature. Ultrathin sections (60–90 nm) were cut with an LKB-8800 ultramicrotome equipped with a diamond knife and mounted on 100-mesh nickel grids coated with 0.3% Formvar films for subsequent immunolabeling.

The ultrathin sections were first blocked by floating the grids on droplets of PBS2 (8 mM Na_2HPO_4, 1.5 mM KH_2PO_4, 3 mM KCl, and 500 mM NaCl, pH 7.4) supplemented with 50 mM Gly for 30 min at room temperature and continuously blocked with PBS2 supplemented with 0.1% (w/v) gelatin, 0.5% (w/v) bovine serum albumin (BSA), and 0.1% (v/v) Tween 20 (pH 7.4)

(PBGT). Without rinsing, the sections were incubated with rabbit antiserum directed either against the grapevine hexose transporter VvHT1or the Arabidopsis plasma membrane H^+-ATPase AHA3 (both diluted 1:100 in PBGT buffer) overnight at 4°C. Following extensive washes with PBGT buffer, the sections were incubated with secondary antibody (goat anti-rabbit IgG antibody conjugated with 10 nm gold) at 1:100 dilution in PBGT buffer for 2 h at room temperature. The sections were rinsed consecutively with PBGT and double-distilled water. The sections were then stained with 2% uranyl acetate in 50% ethanol for 25 min at 25°C and with alkaline lead citrate for 15 min. After extensively washing with double distilled water, the ultrathin sections were examined with a JEM-100S electron microscope.

The specificity and reliability of the immunogold-labeling were tested by two negative controls. In the first one, the antiserum was omitted to test possible unspecific labeling of the goat anti-rabbit IgG antibody-gold conjugate. In the second one, rabbit preimmune serum was used instead of the rabbit antiserum before immunogold labeling to test the specificity of the antiserum. More than three repetitions of the control experiments were conducted for each sample.

SDS-PAGE and Immunoblotting

The subcellular fractions were prepared from the fruit flesh, and the purity of each subcellular fraction was evaluated by measuring the activity of the marker enzymes according to Zhang et al. (1999, 2001a). The plasma membrane, endomembrane, and cytosolic fractions were all of high purity and biochemically active (data not shown). SDS-PAGE and immunoblotting of these subcellular fractions was conducted essentially according to Zhang et al. (2001b). Briefly, after electrophoretic transfer from the polyacrylamide gels, the nitrocellulose membranes were blocked and incubated overnight at 4°C in the antiserum directed either against the grapevine hexose transporter VvHT1 or the Arabidopsis plasma membrane H^+-ATPase AHA3 (both diluted 1:1,000 in the blocking buffer). Following extensive washes, the membranes were incubated with goat anti-rabbit IgG-alkaline phosphatase conjugate. The membranes were stained with 5-bromo-4-chloro-3-indolyl phosphate and nitroblue tetrazolium.

Protein concentrations were determined by the method of Bradford (1976) with BSA as a standard.

$^{14}CO_2$ Labeling

The spur (short shoots bearing fruits) leaves were labeled with $^{14}CO_2$ to follow subsequent movement of radioactivity into fruits. The spur leaves were enclosed in plastic bags, and the radiolabel was injected into a vial inside the bag. Each spur received 1.85 MBq of $^{14}CO_2$ released from [^{14}C]bicarbonate by addition of excess 3 M lactic acid. The leaves were exposed to $^{14}CO_2$ for 1 h before injecting excess 3 M KOH to neutralize the acid and to absorb any remaining $^{14}CO_2$. After labeling, the spurs were left for 18 h to translocate ^{14}C to fruits.

Autoradiography

After $^{14}CO_2$ labeling, fruit tissue for autoradiography was selected and sectioned before rapid freezing in liquid nitrogen between sheets of paper. The frozen sample was gently compressed between aluminum plates and freeze-dried. After drying, the tissue was pressed flat and autoradiographed using Kodak BioMax MR-1 film (Sigma, Poole, UK) at −80°C for 5 d.

[^{14}C]Sorbitol Unloading Experiments

Five-year-old potted apple trees grown in a fully conditioned green house were used. The experiment was conducted at 28°C unless otherwise stated. [^{14}C]sorbitol (2×10^5 Bq mL^{-1}), PCMBS (1 mM) or Na_3VO_4 (0.5 mM) were dissolved in a buffer (buffer A) containing 50 mM K_2HPO_4-KH_2PO_4 (pH 7.2), 10 mM $CaCl_2$, 10 mM EDTA, and 400 mM Suc. Anti-VvHT1 serum, anti-AHA3 serum, or rabbit preimmune serum were diluted 1:500 in the same buffer. [^{14}C]sorbitol was continuously introduced into the fruit from the pedicel by a method similar to that used for CFDA supply (Fig. 1) where the phloem zone of the pedicel was gently scratched with a small knife, and the solution (0.1 mL) was quickly applied by a special silicon bag covering the phloem zone. The [^{14}C]sorbitol unloading in the fruits was evaluated by an unloading trap technique that was originally developed by Oparka and Prior (1987) in potato tubers and previously used in apple fruits in our laboratory (Lu et al., 1999). Small wells were made into the fruit using a 10-mm-diameter cork borer 4 h after the [^{14}C]sorbitol feeding. The positions of these wells, relative to the sepal bundles, are shown in Figure 8. Three wells were made in each fruit, approximately 1.5 cm apart (Fig. 8A), with one well for the treatments by the reagents and two others for the controls. A solution (1–2 mL) containing 600 mM mannitol, 1 mM $CaCl_2$, 0.4% (w/v) Macerozyme (Yakult R-10), 1% (w/v) cellulase (Onozuka R-10), 0.1% (w/v) polyvinylpyrrolidone 40, 0.2% (w/v) BSA, and 20 mM MES-NaOH (pH 5.6) was added to the treatment wells and one of the two control wells. After a short enzymatic digestion of the flesh tissues for 15 min, solution was discarded and the wells were washed by the buffer A described above. The solution containing PCMBS, Na_3VO_4, anti-VvHT1 serum, anti-AHA3 serum or rabbit preimmune serum were added into the treatment wells, and the same buffer (buffer A) containing none of these reagents into one of the control wells. After a 20-min treatment at 25°C, these solutions were removed and the wells were briefly washed with the unloading medium containing 20 mM MES-NaOH (pH 6.8), 2 mM $CaCl_2$, 2 mM $MgCl_2$, 1 mM KH_2PO_4, and 50 mM polyethylene glycol (PEG) 200. Fresh unloading medium (1–2 mL) was then added into the wells. Another control well received only the unloading medium without any other treatments described above. So, one set of experiments consisted of seven fruits. The unloading medium was collected 1 h after incubation in the well, and the well-tissue (about 0.5 g) was also sampled for analysis. The sampling positions in the wells are shown in Figure 8B. The radioactivity was directly counted in the collected unloading medium. The well-tissues sampled were quickly washed with the fresh unloading medium, sectioned, extracted, and finally counted for radioactivity. The same unloading experimental procedures for each well were repeated two times, and the periods of the measured unloading corresponded approximately to 5 to 6 h, 7 to 8 h, and 9 to 10 h after the [^{14}C]sorbitol feeding from the pedicel.

Distribution of Materials

Upon request, all novel materials described in this publication will be made available in a timely manner for noncommercial research purposes, subject to the requisite permission from any third-party owners of all or parts of the material. Obtaining any permissions will be the responsibility of the requestor.

ACKNOWLEDGMENTS

We thank Dr. R. Serrano (Universidad Politecnica de Valencia, Instituto de Biología Molecular y Celular de Plantas (IBMCP), 46022 Valencia, Spain) for his generous gift of the antibody raised against the Arabidopsis plasma membrane H^+-ATPase AHA3. We also thank Dr. A. Roberts (Scottish Crop Research Institute, Tayside, Scotland) for his generous gift of Texas Red and kind guidance in the use of this chemical.

Received November 23, 2003; returned for revision February 10, 2004; accepted February 25, 2004.

LITERATURE CITED

Baluska F, Cvrckova F, Kendrick-Jones J, Volkmann D (2001) Sink plasmodesmata as gateways for phloem unloading. Plant Physiol **126:** 39–46

Beruter J, Studer FME, Ruedi P (1997) Sorbitol and sucrose partitioning in the growing apple fruit. J Plant Physiol **151:** 269–276

Bradford MM (1976) A rapid and sensitive method for the quantitation of microgram quantities of protein utilizing the principle of protein-dye binding. Anal Biochem **72:** 248−254

Brown SC, Coombe BG (1985) Solute accumulation by grape pericarp cells. III. Sugar changes in vivo and the effect of shading. Biochem Physiol Pflanz (BPP) **180:** 371–381

Buttner M, Sauer N (2000) Monosaccharide transporters in plants: structure, function and physiology. Biochim Biophys Acta **1465:** 263–274

Dennis FG (1986) Apple. *In* SP Monselise, ed, CRC Handbook of Fruit Set and Development. CRC Press, Boca Raton, FL, pp 1–44

Ellis EC, Turgeon R, Spanswick RM (1992) Quantitative analysis of photosynthate unloading in developing seeds of *Phaseolus vulgaris*. III. Pathway and turgor sensitivity. Plant Physiol **99:** 644–651

Fieuw S, Patrick JW (1993) Mechanism of photosynthate efflux from *Vicia faba* L. seed coats. I. Tissue studies. J Exp Bot **44:** 63–74

Fieuw S, Willenbrink J (1991) Isolation of protoplasts from tomato fruit (*Lycopersicon esculentum*): first uptake studies. Plant Sci **76:** 9–17

Fillion L, Ageorges A, Picaud S, Coutos-Thevenot P, Lemoine R, Romieu C, Delrot S (1999) Cloning and expression of a hexose transporter gene expressed during the ripening of grape berry. Plant Physiol **120:** 1083–1093

Fisher DB, Oparka KJ (1996) Post-phloem transport: principles and problems. J Exp Bot **47:** 1141–1154

Gao Z, Maurousset L, Lemoine R, Yoo SD, van Nocker S, Loescher W (2003) Cloning, expression, and characterization of sorbitol transporter from developing sour cherry fruit and leaf sink tissues. Plant Physiol **131:** 1566–1575

Harrison MJ (1996) A sugar transporter from *Medicago truncatula*: altered expression pattern in roots during vesicular-arbuscular (VA) mycorrhizal association. Plant J **9:** 491–503

Haupt S, Duncan GH, Holzberg S, Oparka KJ (2001) Evidence for symplastic phloem unloading in sink leaves of barley. Plant Physiol **125:** 209–218

Hayes PM, Patrick JW, Offler CE (1987) The cellular pathway of radial transfer of photosynthates in stems of *Phaseolus vulgaris* L.: effect of cellular plasmolysis and p-chloromercuribenzenesulfonic acid. Ann Bot (LOND) **59:** 635–642

Imlau A, Truenit E, Sauer N (1999) Cell-to-cell and long-distance trafficking of the green fluorescent protein in the phloem and symplastic unloading of the protein into sink tissue. Plant Cell **11:** 309–322

Itaya A, Ma F, Qi Y, Matsuda Y, Zhu Y, Liang G, Ding B (2002) Plasmodesma-mediated selective protein traffic between ''symplasmically isolated'' cells probed by a viral movement protein. Plant Cell **14:** 2071–2083

Kempers R, Ammerlaan A, van Bel AJE (1998) Symplasmic constriction and ultrastructural features of sieve element/companion cell complex in the transport phloem of apoplasmically and symplasmically phloem-loading species. Plant Physiol **116:** 271–278

Knoblauch M, van Bel AJE (1998) Sieve tubes in action. Plant Cell **10:** 35–50

Koch KE, Avigne WT (1990) Post-phloem, nonvascular transfer in citrus: kinetics, metabolism, and sugar gradients. Plant Physiol **93:** 1405–1416

Kuhn C, Hajirezaei MR, Fernie AR, Roessner-Tunali U, Czechowski T, Hirner B, Frommer WB (2003) The sucrose transporter *StSUT1* localizes to sieve elements in potato tuber phloem and influences tuber physiology and development. Plant Physiol **131:** 102–113

Lang A, During H (1991) Partitioning control by water potential gradients: evidence for compartmentation breakdown in grape berries. J Exp Bot **42:** 1117–1123

Lang A, Ryan KG (1994) Vascular development and sap flow in apple pedicels. Ann Bot (Lond) **74:** 381−388

Loescher WH (1987) Physiology and metabolism of sugar alcohols in higher plants. Physiol Plant **70:** 553−557

Lu YM, Zhang DP, Yan HY (1999) Sugar unloading mechanisms in the developing apple fruit. Acta Hortic Sin **26:** 141−146

Offler CE, Patrick KJ (1993) Pathway of photosynthate transfer in the developing seed of *Vicia faba* L.: a structural assessment of the role of transfer cells in unloading from the seed coat. J Exp Bot **44:** 7117–7124

Oparka KJ (1990) What is phloem unloading? Plant Physiol **94:** 393–396

Oparka KJ, Prior DAM (1987) ^{14}C sucrose efflux from the perimedulla of growing potato tubers. Plant Cell Environ **10:** 667–675

Oparka KJ, Prior DAM, Wright KM (1995) Symplastic communication between primary and developing lateral roots of *Arabidopsis thaliana*. J Exp Bot **46:** 187–199

Oparka KJ, Santa Cruz S (2000) The great escape: phloem transport and unloading of macromolecules. Annu Rev Plant Physiol Plant Mol Biol **51:** 323–347

Oparka KJ, Turgeon R (1999) Sieve elements and companion cells-traffic control centers of the phloem. Plant Cell **11:** 739–750

Pardo JM, Serrano R (1989) Structure of a plasma membrane H^+-ATPase gene from the plant *Arabidopsis thaliana*. J Biol Chem **264:** 8557–8562

Patrick JW (1997) Phloem unloading: sieve element unloading and post-sieve element transport. Annu Rev Plant Physiol Plant Mol Biol **48:** 191–222

Patrick JW, Offler CE (1996) Post-sieve element transport of photoassimilates in sink regions. J Exp Bot **47:** 1165–1177

Patrick JW, Offler CE, Wang XD (1995) Cellular pathway of photosynthate transport in coats of developing seed of *Vicia faba* L. and *Phaseolus vulgaris* L. I. Extent of transport through the coat symplast. J Exp Bot **46:** 35–47

Roberts AG, Santa Cruz S, Roberts IM, Prior DAM, Turgeon R, Oparka KJ (1997) Phloem unloading in sink leaves of *Nicotiana benthamiana*: comparison of a fluorescent solute with a fluorescent virus. Plant Cell **9:** 1381–1396

Ruan YL, Patrick JW (1995) The cellular pathway of post-phloem sugar transport in developing tomato fruit. Planta **196:** 434–444

Schmalstig JG, Cosgrove DJ (1990) Coupling of solute transport and cell expansion in pea stem. Plant Physiol **94:** 1625–1634

Schulz A (1998) Phloem: structure related to function. Prog Bot **59:** 430–447

Sonnewald U, Hajirezaei MR, Kossmann J, Heyer A, Tretehwey RN, Willmitzer L (1997) Increased potato tuber size resulting from apoplastic expression of a yeast invertase. Nat Biotechnol **15:** 794–797

van Bel AJE (1996) Interaction between sieve element and companion cell and the consequences for photoassimilate distribution: two structure hardware frames with associated physiological software packages in dicotyledons. J Exp Bot **47:** 1129–1140

Viola R, Roberts AG, Haupt S, Gazzani S, Hancock RD, Marmiroli N, Machray GC, Oparka KJ (2001) Tuberization in potato involves a switch from apoplastic to symplastic phloem unloading. Plant Cell **13:** 385–398

Wang XD, Harrington G, Patrick JW, Offler CE, Fieuw S (1995a) Cellular pathway of photosynthate transport in coats of developing seed of *Vicia faba* L. and *Phaseolus vulgaris* L. II. Principal cellular site(s) of efflux. J Exp Bot **46:** 49–63

Wang HL, Offler CE, Patrick JW (1995b) The cellular pathway of photosynthate transfer in the developing wheat grain. II. A structural analysis and histochemical studies of the pathway from the crease phloem to the endosperm cavity. Plant Cell Environ **18:** 373–388

Wright KM, Oparka KJ (1997) Metabolic inhibitors induce symplastic movement of solutes from the transport phloem of *Arabidopsis* roots. J Exp Bot **48:** 1807–1814

Yamaki S, Ino S (1992) Alteration of cellular compartmentation and membrane permeability to sugars in immature and mature apple fruit. J Am Soc Hortic Sci **117:** 951–954

Zhang DP, Chen SW, Peng YB, Shen YY (2001a) Abscisic acid-specific binding sites in the flesh of developing apple fruit. J Exp Bot **52:** 2097−2103

Zhang DP, Lu YM, Wang YZ, Duan CQ, Yan HY (2001b) Acid invertase is predominantly localized to cell walls of both the practically symplasmically isolated element/companion cell complex and parenchyma cells in developing apple fruits. Plant Cell Environ **24:** 691–702

Zhang DP, Wang YZ (2002) Post-translational inhibitory regulation of acid invertase induced by fructose and glucose in developing apple fruit. Sci China Ser C Life Sci **45:** 309–321

Zhang DP, Zhang ZL, Chen J, Jia WS (1999) Specific abscisic acid-binding sites in mesocarp of grape berry: properties and subcellular localization. J Plant Physiol **155:** 324−331